Image Analysis in Quantitative Particle Studies of Archaeological Ceramic Thin Sections

Chandra L. Reedy, Jenifer Anderson, Terry J. Reedy, and Yimeng Liu

This paper presents the results of experimental research into optimal protocols for the use of image analysis as a tool for obtaining quantitative data on ceramic thin sections. While qualitative examination of thin sections under the microscope will always remain crucial for mineral identification, for many textural characterizations, and for comparing mineralogy to geological data, digital image analysis can provide important data for quantitative studies. Here we focus on the analysis of aplastic inclusions. We first experimented with a variety of software options. We then developed protocols that proved fast and reliable in providing consistent results for obtaining area percentage of components, as well as simultaneously giving data on size and shape characteristics. Through initial analysis of laboratory-

ABSTRACT

Thin-section petrography is a crucial tool for the study of archaeological ceramics, and in recent years, image analysis has emerged as a powerful quantitative enhancement of that tool. Exploratory applications of image analysis to archaeological ceramic thin sections, and related work by sedimentary geologists, have indicated its usefulness to the field. In this paper, we first present the results of experimental work testing the consistency and reproducibility of image analysis. We identify procedures for fast and reliable analysis of thin sections using laboratory-prepared ceramic specimens of simple clay-sand systems. We then show how those procedures can be slightly modified to accommodate more complex archaeological specimens. We conclude with a discussion of the role of image analysis within the overall context of thin-section petrography of ceramic materials, as one among a repertoire of techniques, adding quantitative data and increasing the usefulness of ceramic thin sections for addressing archaeological research questions.

La petrografía de lámina delgada constituye una herramienta fundamental para el estudio de cerámicas arqueológicas y en los últimos años, ha surgido el análisis de imágenes como una mejora cuantitativa importante para dicha herramienta. El uso exploratorio del análisis de imágenes en láminas delgadas de cerámicas arqueológicas, junto con trabajos relacionados realizados por sedimentólogos, han demostrado su utilidad en ese campo. En este trabajo presentamos en primer lugar los resultados de investigación sobre la consistencia y reproducibilidad del análisis de imágenes. Identificamos los procedimientos para el análisis rápido y confiable de láminas delgadas, utilizando muestras de cerámica preparadas en laboratorio a partir de sistemas arcillo-arenosos simples. Luego mostramos cómo estos procedimientos pueden ser ligeramente modificados para adecuarse a muestras arqueológicas más complejas. Finalizamos con una discusión sobre el rol del análisis de imágenes dentro del contexto general de la petrografía de lámina delgada de cerámicas, como una entre muchas técnicas, que agrega datos cuantitativos e incrementa la utilidad de las láminas delgadas de cerámicas para abordar estudios de investigación arqueológica.

Advances in Archaeological Practice 2(4), 2014, pp. 252–268
Copyright 2014© The Society for American Archaeology
DOI: 10.7183/2326-3768.2.4.252

prepared specimens focusing on sand-tempered ceramics, we developed and tested procedures. We then extended this work to a variety of other particles typically found in archaeological ceramics, seeing if and how adjustments are needed for certain materials. Although not a major focus of this paper, we also discuss the use of image analysis to study porosity in ceramic thin sections. We show how image analysis can be integrated into thin-section petrography routines to enrich any archaeological ceramic research with a wide range of quantitative data.

Thin-section petrography is a long-standing method for characterizing archaeological ceramics and investigating research questions concerning ceramic production, function, exchange, technological style, and use history (Peacock 1970; Quinn 2009, 2013; Reedy 2008; Shepard 1971; Williams 1983). Traditional thin-section petrography involves qualitative examination and mineral identification under a polarizing light microscope, augmented with quantitative data collected with the aid of a stage or eyepiece micrometer and/or a point-counting stage and recording tool. Newer analytical methods (such as scanning electron microscopy with elemental analysis capabilities), while providing alternative ways of examining and understanding ceramic materials, have not eliminated the importance of this earlier method. Thin sections are used to identify and quantify aplastic inclusions, at times even making it possible to deduce geological source parameters of minerals and rock fragments; to characterize textures and fabrics related to production and firing regimes, pore structures, alteration products, and matrix characteristics; and to study decorative surfaces and interfaces between the ceramic body and slip or glaze layer (Arnold 1972; Day and Wilson 1998; Dickinson and Shutler 1979; Freestone et al. 1982; Middleton and Freestone 1991; Quinn 2009, 2013; Reedy 2008; Rice 1987; Rye 1976; Stoltman 2001; Velde and Druc 1999; Whitbread 1995). This paper focuses specifically on the quantitative study of aplastic inclusions in ceramic bodies. These particles may be natural components of clays but are often added as temper materials to improve working, drying, firing, and functional characteristics of ceramics.

Sand is commonly encountered in archaeological ceramics. It consists primarily of quartz (but may also have varying amounts of feldspars, micas, iron oxides and other minerals, and rock fragments), and it can be either a natural component and/or an additive. Sand is also defined by grain size, with several competing classification schemes. In the United States, sedimentary geologists often use the Udden-Wentworth scale (Udden 1914; Wentworth 1922), which defines sand as consisting of particles between .063 and 2.0 mm. Smaller particles between .004 and .063 mm are called silt; clay is defined as having a particle size less than .004 mm. International standards developed for soil classification in the engineering field also define sand as between .063 and 2.0 mm, but put silt at .002-.063 mm and clay as less than .002 mm (Norbury 2010).

The presence of larger particles can be beneficial to the working, drying, firing, and functional properties of clay (Rice 1987). The amount of sand, and the size and shape characteristics of grains, may be useful in characterizing the geological deposit exploited by a workshop and in distinguishing that workshop's products from those of other workshops. Crushed rock fragments, shell, crushed sherds (grog), or organic materials such as straw are also typical temper additives used instead of, or in addition to, sand.

Traditionally, several approaches have been used to obtain quantitative data on the amount, size, or shape of particles in petrographic thin sections of ceramics. For amount, estimates or manual counts of area percentage are obtained. One approach is to make visual estimations using comparison charts (Matthew et al. 1991; Rice 1987:349). For shapes, sedimentary geologists have developed images to estimate the shape of quartz grains (Pettijohn 1975). Another approach is to do point counting, where the relative proportion of different minerals or features is counted for each of many fields of view by recording what appears at the intersections along a superimposed grid (Hutchison 1974; Middleton et al. 1985; Stoltman 1989). In addition to counting particle types, one can include size measurements at each intersection using a micrometer or eyepiece graticule to measure each individual grain to identify a range and average size. Shape characteristics can be included by taking both length and width measurements.

Visual estimation has the advantage of being relatively fast, so it is feasible to include many thin sections and thus improve statistics; however, accuracy and reproducibility are not as good as with the more careful but time consuming point counting and individual measurement method. In point counting, a large number of points need to be included for statistical validity. The exact number needed varies depending on the nature of the material and the purpose of the study. For example, if one is trying to capture information on all possible accessory minerals present, more points will be needed than if the goal is simply to quantify the relative abundance of the most common minerals. The main goal in point counting is that one wants to make sure that enough points are counted that any further counting can be expected to have a negligible effect on results (Fieller and Nicholson 1991; Leese 1983; Orton 2000; Streeten 1982). While some geologists find that counting 1000-2000 points may be necessary to achieve that goal (Hutchison 1974), ceramic petrographers more often find 100-300 points to be sufficient (Quinn 2013; Stoltman 2001).

However, these 100-300 points most often must be counted on multiple thin sections. Freestone (1995) notes that, while in some circumstances only a single thin section may suffice to predict the geological source of rock and mineral inclusions (as in cases in which inclusions came from a single outcrop of unusual composition), in cases in which differences between ceramic groups are subtle, sample sizes sufficient for a reliable provenance study are necessary (often 10 or more thin sections per group). Making hundreds of individual measurements on a large number of thin sections can require many hours of labor for each thin section. Hence sedimentary geologists and ceramic petrographers alike have explored the incorporation of image analysis into their work.

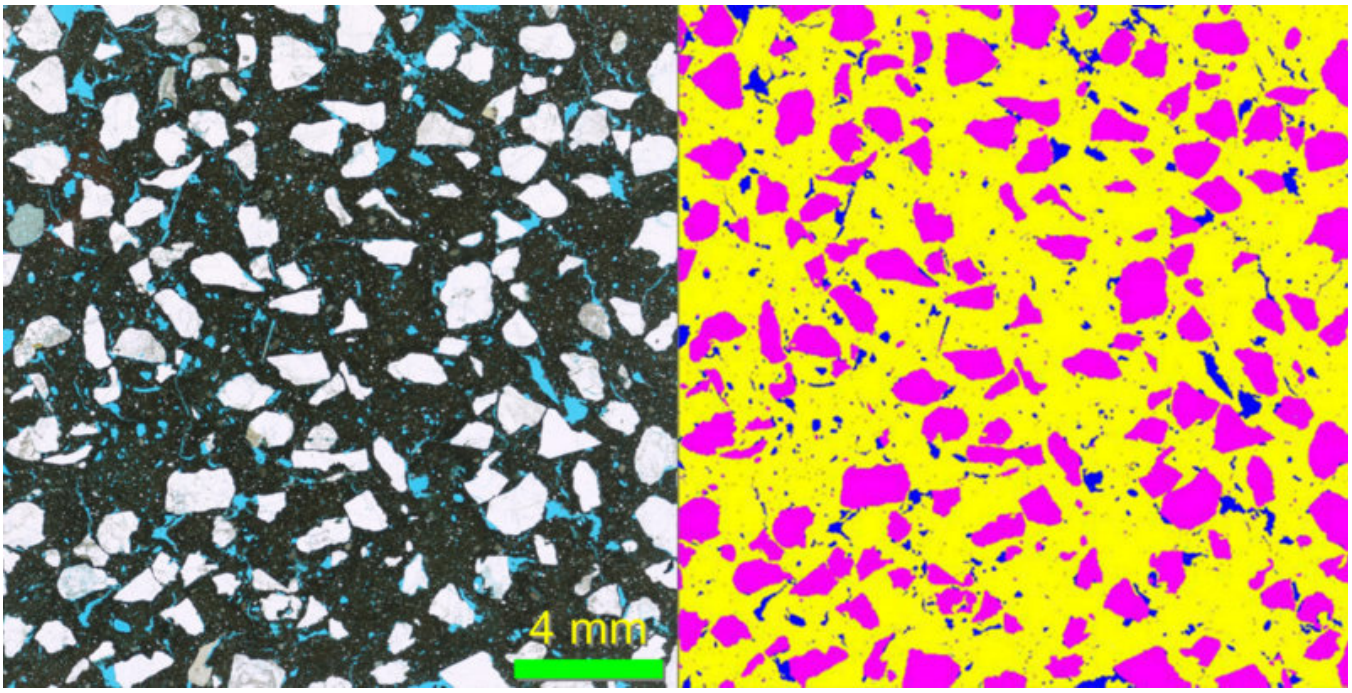

FIGURE 1. Left: scanned image of laboratory-prepared specimen with 16-mesh sand, 40 percent by volume, kneaded into wet clay, with the sand grains appearing white, pores blue, and clay matrix brown. Right: the segmentation process has marked the sand and silt in pink, the pores in dark blue, and the clay matrix in yellow. Once the components are correctly identified by the image analysis program, any number of size and shape characteristics can be obtained simultaneously.

IMAGE ANALYSIS IN THIN-SECTION PETROGRAPHY

The main idea of digital image analysis is to enhance visual separation of different components in a thin section and then to highlight, or mark for analysis, certain components of a specific color, contrast, size range, and/or morphology (Figure 1). This process is called "segmentation." Satisfactory segmentation is the core requirement for successful image analysis. Once this is achieved, a wide variety of data on those highlighted particles can then be gathered by the analysis program simultaneously, depending on the needs of the research project (e.g., number of grains, area percentage, range and average size, degree of roundness, aspect ratio, range and average length of axes, length of perimeter, etc.).

For each group of ceramics, specific protocols for differentiating the particles of interest may be needed, depending on the appearance of the matrix and how well each component to be segmented stands out from other components and from the matrix itself. Each type of non-matrix grain can be segmented separately in sequence, or multiple components can be segmented at once. Decisions then need to be made regarding what data should be collected on those particles in order to answer specific research questions.

Since soils, sands, and sandstones have similarities to ceramic materials, research on image analysis by sedimentary geologists is relevant to ceramic studies. Schäfer and Teyssen (1987) pioneered an image analysis system to determine grain-size distribution, grain shape, and grain orientation in thin sections of sands and sandstones. Protz and VandenBrygaart (1998) developed a protocol for using image analysis to differentiate pores, organic matrix, clay coatings, and carbonate and iron concretions in thin sections of soils. Francus (1998) showed how image analysis (using a binary conversion process) to examine grain size variation in thin sections of soft clastic sediments can be done relatively quickly and quantitatively.

Image analysis has also been used by sedimentary and engineering geologists to obtain quantitative data on particle shape (Coster and Chermant 2001). Tafesse et al. (2013) evaluated image analysis protocols for quantifying particle angularity, considered a crucial parameter to measure because it relates to the transport history of particles in sedimentary deposits. They noted that visual charts previously used to estimate angularity are subjective and time-consuming, so they tested and ranked several image analysis methods. Although they did not end up recommending any of them, they did lay out some ideas for the next steps of research. Possible sources of errors to be avoided in image analysis characterizations of size, length, perimeter, and shape are outlined by Schäfer (2002). Other morphological parameters carrying useful geological information routinely and accurately acquired by image analysis include feret diameter (also known as length, or caliper length along the major axis); circularity (the ratio of the area of an object against a circle whose maximum diameter is equal to the object's maximum feret); aspect ratio (ratio of the largest diameter of a grain to the smallest); and roundness (relates the area of a grain to its perimeter) (Cox and Budhu 2008; Persson 1998). Many other

parameters are also available and may be useful for specific research questions.

For ceramics, the area percentage of aplastic inclusions (natural or added) provides information about the original material chosen by the potters and may help to characterize a workshop or ware type according to the preferred material. For example, Wolf (2002) studied aplastic inclusions in brick using quantitative image analysis of thin sections (with IMAGENIA software). Analyzing five images (five fields of view under the microscope) per thin section (with 13 thin sections comprising three production sites), total particle counts were obtained, along with the mean volume (area) percentages of inclusions > .015 mm. Significant differences in the percentage of inclusions were found between the three sites.

Schmitt (1993) used image analysis to characterize thin sections of Roman amphoras found in Lyons, France. She calculated the percentage of particles and the grain-size distribution for aplastic inclusions, summing the results obtained under the microscope from 10 fields of view for each thin section. Velde and Druc (1999) and Bouchain and Velde (2001) used image analyses of common-ware sherds from central France to measure the amount of aplastic inclusions present and to assess grain size distributions. Photomicrographs of thin sections were scanned and then processed to enhance aplastic inclusions (mainly quartz, feldspar, and white micas) using a binary conversion process to convert the grains to black and the clay background to white. They then used an in-house image analysis program and a spreadsheet to compute area percentage and examine frequency of various grain diameters. Other early experiments with applying image analysis to studies of particles in ceramics include work by Streeten (1982), Fieller and Nicholson (1991), Whitbread (1991), and Forte (1994).

Image analysis is also used to characterize pore size, abundance, and patterning in ceramic materials. Although not the primary focus of this paper, our protocol was intended to facilitate analysis of pores. These can form in a number of different ways during pottery production and provide information about fabrication methods and intended function. Thus, for some research questions, characterizing the porosity of a ceramic is useful (Quinn 2013; Reedy 2008; Rice 1987; Rye 1976). The key to using ceramic thin sections for porosity studies (Reedy et al. 2014) is to use a dyed epoxy resin to impregnate and mount the specimen onto the glass slide; pores then easily stand out in plane-polarized light and can be quickly segmented for image analysis. We use a blue-dyed epoxy, but others have used red, or a fluorescent dye if a fluorescent lamp is available on the microscope. The dyed epoxy also facilitates measurement of colorless minerals because it makes it easy to distinguish them from pores.

While these and other initial uses of image analysis in ceramic studies provide a good foundation and indicate that useful data can be derived, they leave some unanswered questions that this work was designed to address. How consistent and reproducible are ceramic image analysis measurements? How many fields of view are needed, or how large should the area be, for a reliable analysis? Are there alternatives to using microscope fields of view? Are there protocols that can take advantage of current advances in image analysis programs to improve the ease, speed, and reliability of image analysis for projects involving large numbers of thin sections? Finally, what is the role of image analysis within the overall context of thin-section petrography of ceramic materials?

PREPARATION OF EXPERIMENTAL UNITS

We began developing and testing protocols using laboratory-prepared specimens with simple systems made of clay with a quartz-rich sand additive. Two types of clay were used—a red earthenware that fires to a deep orange red (Earthen Red from Clay-King) and a gray earthenware that fires to a white color (White Earthenware from Clay-King)-to give two very different visual appearances for the image analysis work. We picked three size ranges of sand (from Mile Hi Ceramics): coarse (16-mesh), medium (30-mesh), and fine (70-mesh). The fine and medium sands were primarily quartz, with accessory iron oxides. The coarse sand also had a minor feldspar component. Each was then added to the clays in three different target proportions (10, 25, and 40 percent by volume of loose sand into wet clay). After kneading to mix well, each clay-sand mixture was rolled out to an even thickness, and specimens of a standard size were cut out with a cookie cutter-like mold. After thorough drying, they were then fired to the temperature recommended for the clays (900-1000° C), with a gradual increase in temperature over the course of a day.

For each sand percentage, size, and clay combination, five replicate specimens were made, for a total of 90 specimens with added sand. Another six specimens were prepared with no sand additive (three replicates of each clay) to check for background sand. A thin section was then prepared for each of these 96 experimental specimens.

Using a dyed epoxy to impregnate and mount thin sections in a sample highlights the pores. Otherwise, with clear epoxy, pores are colorless like the ubiquitous quartz in plane-polarized light and dark like many grains in crossed-polarized light. Hence, a dyed epoxy is the key for being able to correctly segment particles from pores; we used a blue-dyed epoxy.

Additional replicates of these same materials were examined as surface specimens, rather than in thin section, to assess how much information image analysis can provide on whole samples examined under a stereomicroscope without the extra work of preparing thin sections. This possibility was considered because sherds themselves, especially fresh edges or cleaned surfaces, have been used to obtain some quantitative data supplementing thin-section microscopy (Nijboer et al. 2006). An advantage is that the time and expense of thin-section cutting, mounting, and grinding would be eliminated, allowing data to be collected on even larger numbers of specimens.

We found that we needed a freshly cut area to best see the mineral grains and pores, and so the ceramic specimens were cut using a diamond-edge saw blade. We then captured digital images of a fresh edge viewed under an optical zoom microscope and applied image analysis. While the sand grains were readily visible, and with some effort could be used for image analysis, the pores in the whole specimens were difficult to distinguish. They could not adequately be separated even using

a variety of preprocessing methods. It is quite possible that with additional effort during photography—such as utilizing Reflectance Transformation Imaging (RTI)—the pores may become distinguishable. This is certainly a possibility, because Livingood and Cordell (2014) used a form of RTI with three light source angles (with one a ring flash) to discern shell tempers in whole ceramic sherds adequately enough for image analysis. In their technique, camera and sherd were fixed with multiple images collected by using light from different angles. However, we chose instead to focus on thin sections rather than on whole sherds.

Our original idea was to apply measurement protocols to multiple fields of view of a thin section, and then to obtain an average. However, grains touching a border have to be discounted from any measurements other than area percentage because they are at least partially cut off from view. Consequently, they cannot be accurately measured. This reduces the number of grains available for many analyses. Alternatively, images could be taken of multiple fields of view with an approximately 10 percent overlap and then be tiled and stitched together to make a single, large image for analysis. Then, only the grains on the border of that one large image would need to be eliminated. However, this is time-consuming and so not ideal. The software we chose (Image-Pro Premier) can do automatic tiling, whereby one slowly moves the stage through adjacent areas of a thin section and a larger image is gradually tiled together. However, this too takes some time and creates a very large image file. As a result, we continued to search for an alternative method for processing large numbers of samples more quickly, leading to our decision to use entire scanned thin sections.

IMAGES PRODUCED IN A HIGH-RESOLUTION SCANNER

Using a high-resolution scanner produces an image of an entire thin section (Hansen 2000; De Keyser 1999; Tarquini and Armienti 2003). One can then analyze a single image, zooming in as needed to see small grains or pores. That image especially facilitates studies of macrotexture, eliminating the need to photograph multiple fields of view under the microscope. Important information such as percentages, sorting, size and shape average and range, and amount of porosity are obtained for an entire thin section at once.

In sedimentary petrography, a flatbed scanner is combined with image analysis to characterize particles and pores (Van Den Berg et al. 2003). A flatbed scanning system was also used by Miriello and Crisci (2006) to study macro-porosity (pores larger than 62.5 µm) in archaeological and historic mortars. Livingood (2007) and Livingood and Cordell (2009) scanned thin sections of ceramics at 3200 x 1600 pixels per inch (ppi) and applied image analysis to identify and measure classes of particles as part of an investigation into ceramic paste recipes in the Lower Mississippi Valley. At the selected ppi it was not possible to accurately identify particles of very small size. Nevertheless, the results of this approach were promising for distinguishing and characterizing tempers in ceramic materials, so we decided to pursue this line of research.

After experimenting with various scanners, we chose a Plustek OpticFilm 7600i film scanner with optical resolution of 3600 x 3600 ppi (giving a resolution of 7 µm/pixel), which worked well for most image analysis work on coarser ceramics. We moved to a Plustek OpticFilm 120 film scanner (5300 x 5300 ppi and resolution of 5 µm/pixel) for fine-grained ceramics. A 10-mm scale bar scanned under identical conditions was used to spatially calibrate the systems. The scanned images are quite close to plane-polarized images; crossed-polarized views can be obtained, if desired, by adding a polarizing film sheet.

IMAGE ANALYSIS PROTOCOLS

Some digital microscope cameras come equipped with an analysis package; other packages are available commercially, and some are free web-accessible downloads. After experimenting with a variety of programs (Reedy and Kamboj 2003), we selected Image-Pro Plus, distributed by Media Cybernetics, for its ease of use and comprehensive suite of operations relevant to ceramic thin section analyses. More recently, we moved to their upgraded product, Image-Pro Premier. While we found this package most suitable for our materials and research questions, there are many image analysis programs available that we have not had the opportunity to try. Other users may find an alternative package preferable for their needs.

Whichever program is used, issues that need to be considered include (1) calibration of the image capture system so that measurements are in a specific unit, rather than in number of pixels counted; (2) image quality (most analyses require uncompressed file formats such as a Tagged Image File Format, or TIFF, to prevent loss of image quality, and these must be in very good focus); and (3) image adjustment/enhancement (preprocessing) protocols, if difficulty is found in segmentation (Reedy 2006).

We selected the Image-Pro Premier product (introduced in 2012) especially for its Smart Segmentation procedure. It separates, or segments, the objects of interest based on their differences from the background and other objects using a multi-parameter separation algorithm that can include color channels, background correction, and morphological or textural criteria. It allows one to quickly click on and define the reference areas for background and objects of interest in an image; the reference areas are then used to create segmentation masks to count and measure the objects of interest (Figure 2).

The classification is done on pixel level, with the mean value of every reference object (objects of interest and background objects) calculated for every active channel (which can include color channels, as well as morphologically processed or filtered images). A minimum-distance classification is used to classify pixels on the image: the weighted multi-dimensional Euclidian distance is calculated from the value of every pixel on the image to the mean values of objects of interest and background objects. A pixel is then assigned to the class of the closest reference objects.

Upon opening up a typical ceramic image, the first step is to ensure that the image has the appropriate spatial calibration applied, so that measurements are in microns or millimeters

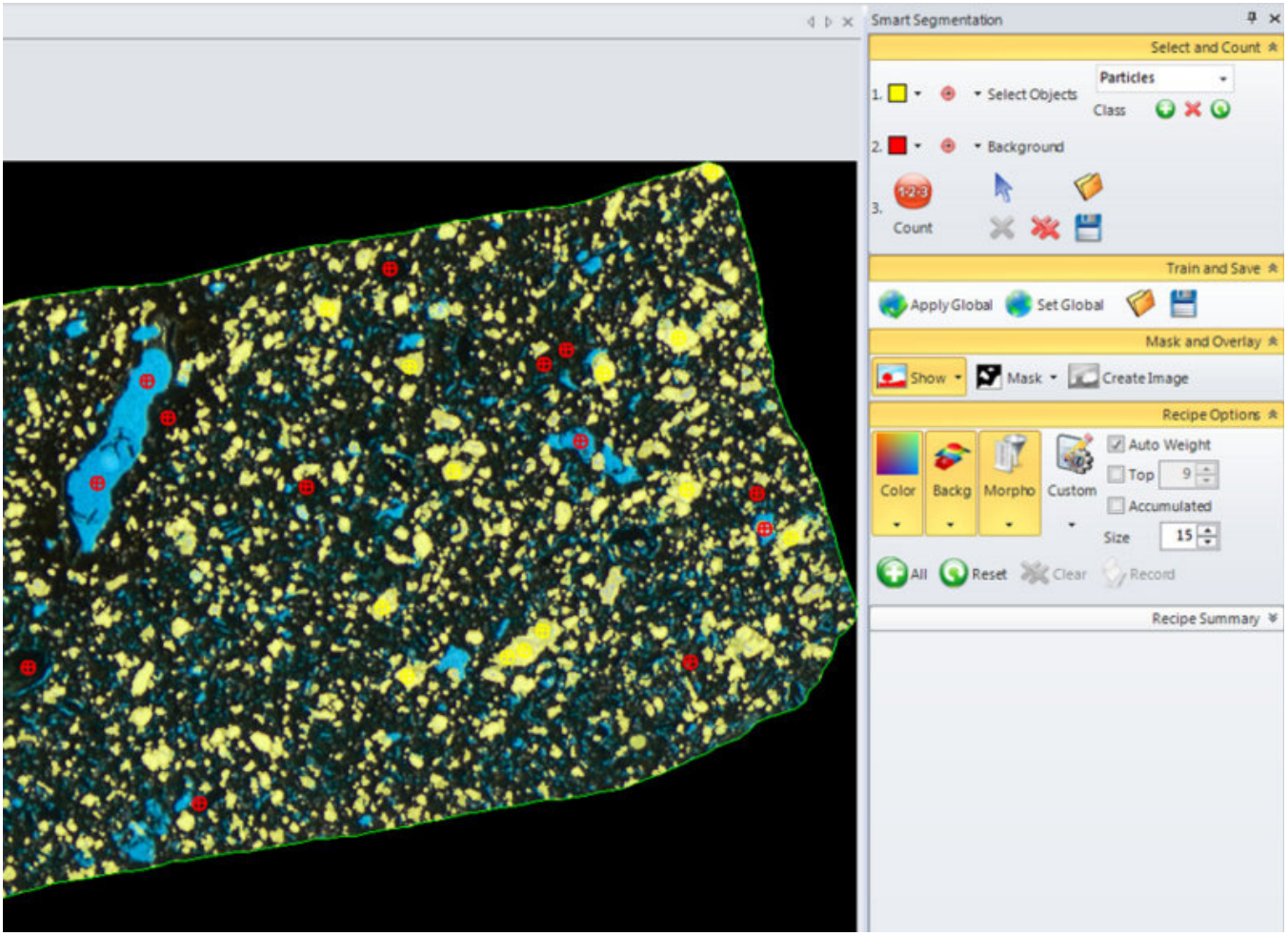

FIGURE 2. The reference marking process in Image-Pro Premier's Smart Segmentation tool. Here, yellow reference marks are placed on sand grains representing the full range of appearances for this class of selected objects, while red marks are used to define the background (in this case both the dark clay matrix and the blue pores). The full suite of color, background, and morphological parameters are included in the minimum-distance classification algorithm. A lightly-tinted yellow overlay interactively displays with each new reference mark what will and will not be included in the selected objects (sand) class, so new reference spots can be added or a previous one removed, as needed.

rather than pixels. To segment the sand grains, one clicks on grains that represent the full range of appearances to set that range as the reference. The background is then set by clicking on clay and pores. If the material is very fine-grained, or has very small pores, zooming in for marking reference points is helpful to ensure that a reference mark covers only the phase intended. Under measurement options, "fill holes" is usually selected, so that if any pixels within a grain are missed in the selection of reference ranges, they will be filled in. The pixel parameters of the background and object areas are then analyzed and a segmentation recipe is created, which includes the parameters giving maximum degree of difference between the objects and background. The segmentation recipe can be saved and applied to a large number of images, as long as they are relatively similar in appearance. This is a huge time saver, because once a reliable segmentation recipe is determine for a material type, it can be reapplied to all similar specimens in that project, eliminating the need to manually mark reference areas for grains and background.

Sometimes the full range of variation that will be encountered in a project is not well represented by a single image, due to differences in paste color or other variables. This variation can occur within a single sherd or across multiple sherds. In that case, a segmentation recipe developed with one thin section may not result in satisfactory segmentation if applied to another thin section. If only a handful of thin sections are affected, preprocessing techniques may suffice to correctly segment those outliers. However, if the variation is more extensive, the Smart Segmentation algorithm can use a series of multiple images to develop the segmentation recipe, so it will work well on all or most thin sections within a project. Sometimes a project may require development of two or more segmentation recipes if there is significant variation.

This segmentation approach generally works well, is fast, and is reproducible (Figure 3). However, when the clay is gray or white, it can sometimes show a slightly blue tint that makes it more difficult to distinguish from the blue of the pores; in this case, prior

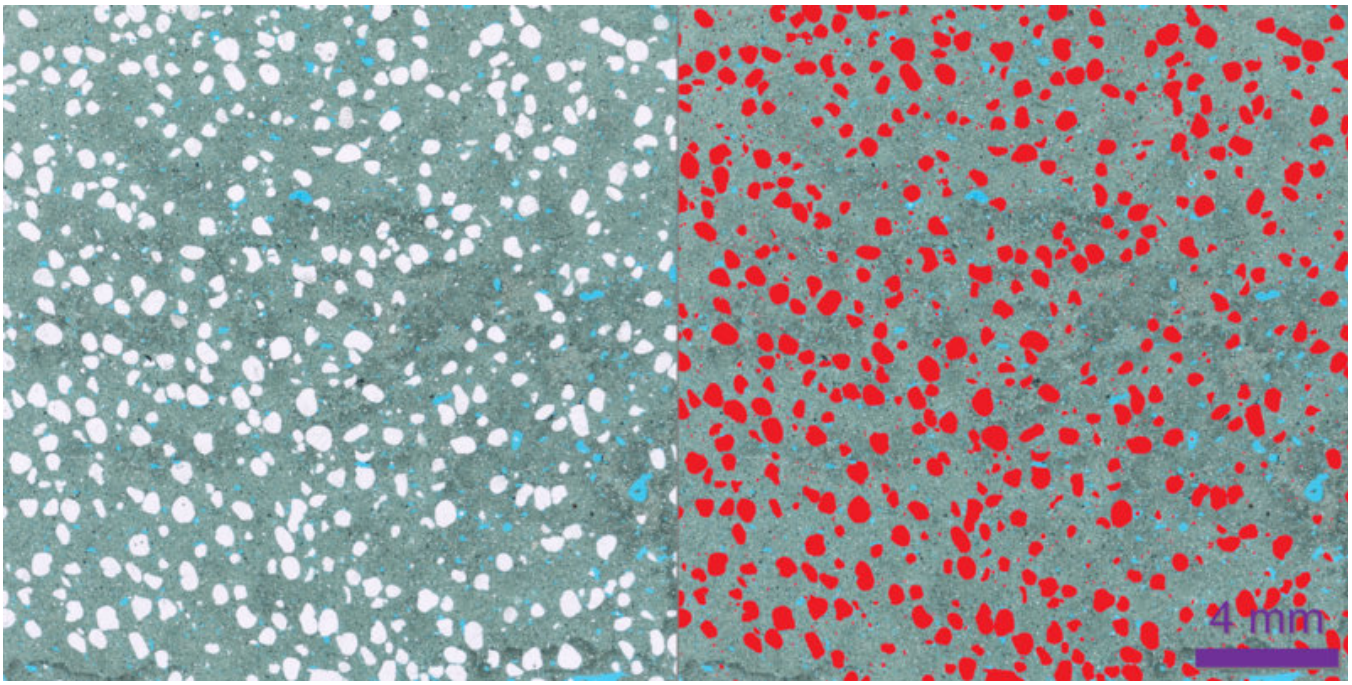

FIGURE 3. Left: scanned image of laboratory-prepared specimen with 30-mesh sand, 25 percent by volume, kneaded into wet clay. Right: with sand grains ≥ .063 mm (21.1 percent) segmented (in red) by a saved recipe.

to segmentation the image can be adjusted in preprocessing to create more contrast between the pores and the matrix for ease of reference marking. We find that lowering the brightness and increasing the contrast sometimes makes the reference marking easier in this case. One could also choose a different color dye for the epoxy for this type of specimen.

In the case of some fine-grained, high-fired ceramics (stoneware and porcelain), while the pores are easily segmented using our standard procedure, we find that sand grain measurements are sometimes more reproducible if we convert the image to monochrome and then proceed with Smart Segmentation. A specific material may require other preprocessing steps (Russ 2011), so some experimentation will be needed at the outset of a project to find the best settings for a fast but reliable procedure (good reproducibility within and between operators).

We also found success with two alternative protocols using the earlier version of Image-Pro software called Image-Pro Plus (Reedy 2012). However, these protocols require more manual steps in preprocessing than is required using the Smart Segmentation tool of the newer Image-Pro Premier software.

If too many of the grains of interest are touching and they are to be measured separately, these can be split by manually drawing a line where the split should occur, or by using automatic splitting tools that can be incorporated into the Smart Segmentation counting procedure. The segmented objects can also be displayed assembled in a separate image, where they are sorted according to any criteria deemed useful, such as length, diameter, area, or aspect ratio (Figure 4). This can help to assess whether joined grains need to be split, to identify a cut-off point for measurements, or to get a better sense of the range represented by the particles in the thin section under study.

Once the component of interest is correctly segmented, any desired measurements can be performed simultaneously. When selecting measurements, start and stop limits can be set to filter out unwanted size or shape categories. For example, for shape characterization we set the size (feret diameter/length) for sand to a .063 mm minimum to filter out silt-sized grains that are often a natural component of clay.

RESULTS OF ANALYSES OF EXPERIMENTAL SPECIMENS

When marking reference areas, Image-Pro Premier allows one to draw circles or other shapes over relatively large areas. However, we found that with archaeological ceramics, doing so may adversely affect segmentation because fine silt-sized particles are often distributed throughout the clay, and there may also be very tiny pores that we want to include in analyses. Hence we often have to use a tool that marks only a single point, to avoid incorporating phases of interest in background marking, which would lead to poor or failed segmentation.

We first tried analyzing the scanned thin sections by selecting reference points for sand particles and background (clay and pores) for each image individually, choosing about 20 reference points total and striving to select the full range of appearance for each component. It is possible to include multiple phases in the same analysis, by marking separate reference points for pores, sand grains, and clay background, for instance. But, given the variation in appearance within each, we found that it was easier to focus on one component at a time (sand particles in this case), and to mark everything else as background. Because different measurement parameters may be selected and saved

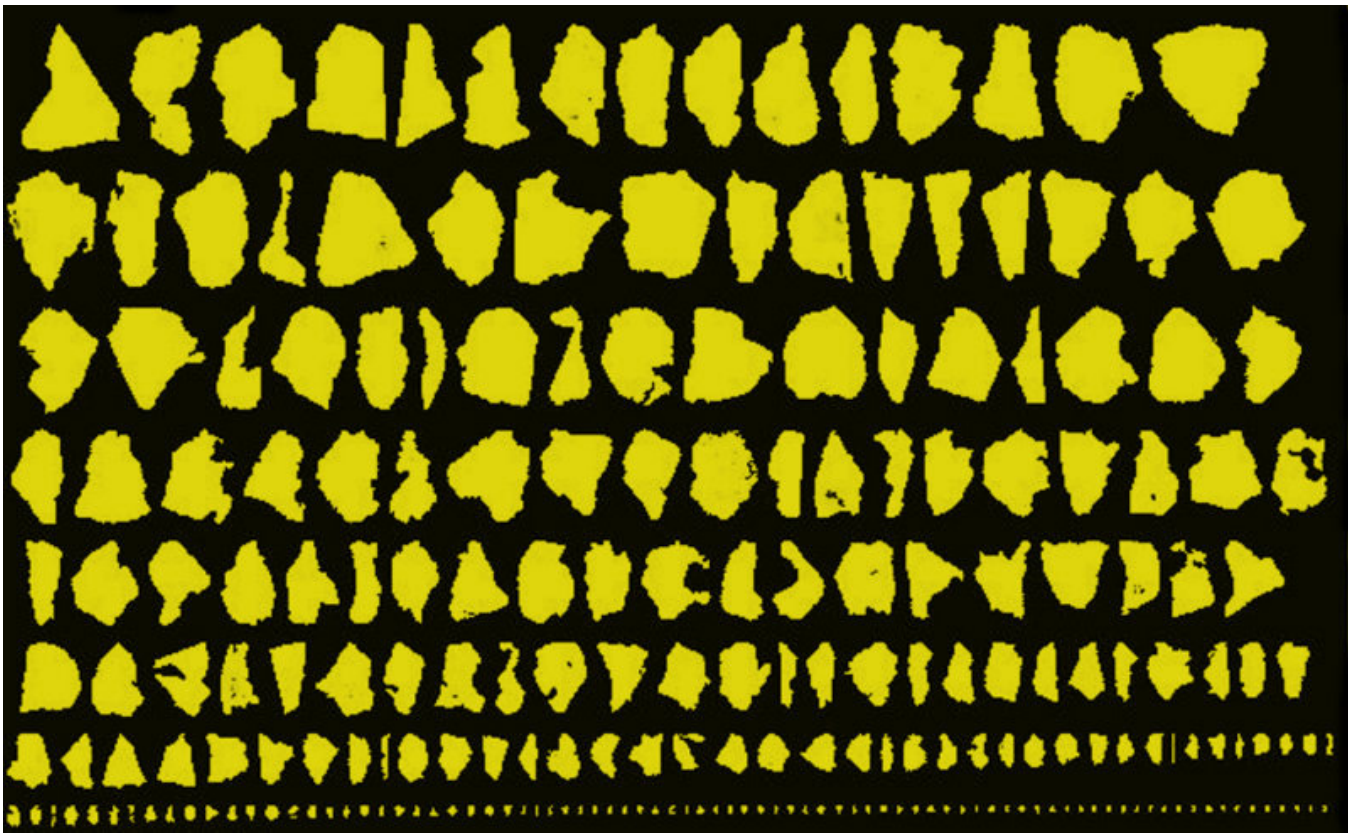

FIGURE 4. The grains in a selected class of objects (in this case sand) in an image can be displayed separately and sorted by any parameter, such as length (as here), diameter, area, aspect ratio, roundness, circularity, etc., to examine the range represented by the particles so as to make sure that there are no joined grains that need to be split, or to identify a good cut-off point for measurements.

for each phase, this procedure seems more efficient. With the ability to save segmentation recipes, it is quite fast to first apply one segmentation recipe for sand and collect that data, and then to apply a second segmentation recipe for pores. In the case of a complex mix of components, segmentation recipes could also be used sequentially to collect relative percentages and measurement data on quartz, feldspars, micas, rock fragments, pores, or any other mix of components that are present.

Table 1 shows a selected group of images that were analyzed by individual reference marking of 10 points each for sand particles and background, repeating the entire procedure three times for each thin section. These analyses were done in random order, rather than having the three repetitions of each image done consecutively, so that a different set of reference points would tend to get selected each time. This table shows that reproducibility of segmentation is excellent.

However, we found that it is very tedious to mark each thin-section image separately. Therefore, we next tried the option in the Smart Segmentation procedure to save a segmentation recipe to reuse on other images. We found that not having to spend time marking each and every image allowed us to focus instead on spending more time being very careful on one representative image (or set of images that bring in the full variation for the project), selecting about 40-60 reference points to construct a segmentation recipe. While the segmentation recipe derived from the red clay worked remarkably well for the white clay, we found that constructing a second one by separately marking reference points for the white clay specimens worked better.

Once the segmentation recipes were developed and saved, analysis of the remaining images proceeded quickly, by simply opening up an image and applying a saved segmentation recipe. The procedure can be automated by constructing macros and using batch processing to (1) sequentially open up each image in a folder, (2) apply the segmentation recipe for sand particles, (3) save the data on pre-selected measurement parameters (summary data and data on each individual particle) into a spreadsheet for statistical analysis, (4) apply segmentation recipes for any other phases to be measured (such as pores) and save that data into a file, and then (5) close out the image and open up the next one. However, for this project, we chose to pause and examine each segmented image to ensure that all visible sand particles were indeed identified without incorrectly marking any background areas. This was done by aligning the segmented image alongside the original image for ease of visual comparison.

Table 2 gives the results for this analysis by carefully constructed segmentation recipe for each of the 96 thin sections of laboratory-prepared specimens. The multiple numbers for each clay type and added sand size/percentage combination represent separate objects, each made from the same batch of clay/sand

TABLE 1. Replication Using 20 Reference Points, Area % Sand-sized Particles (≥ .063 mm)

Sand Approx.%	Red Clay			Mean	σ	White Clay			Mean	σ
Fine, 10	6.5	6.7	6.9	6.7	.2	6.8	6.9	7.0	6.9	.1
Medium, 10	6.3	6.3	6.4	6.3	.1	7.1	7.3	7.5	7.3	.2
Coarse, 10	9.1	9.5	8.6	9.1	.5	7.4	7.0	7.2	7.2	.2
Fine, 25	16.0	15.3	15.3	15.5	.4	18.8	17.2	17.8	17.9	.8
Medium, 25	15.7	16.2	16.2	16.0	.3	20.1	20.4	19.4	20.0	.5
Coarse, 25	20.4	21.0	19.6	20.3	.7	21.4	19.9	19.6	20.3	1.0
Fine, 40	33.1	31.9	33.2	32.7	.7	33.6	31.7	31.5	32.3	1.2
Medium, 40	34.9	35.8	36.2	35.6	.7	33.7	32.0	33.2	33.0	.9
Coarse, 40	31.4	31.4	31.1	31.3	.2	33.2	33.0	32.3	32.8	.5

Note: Segmentation of each thin section was repeated three times (using entire scanned thin section). Twenty reference points selected each time (10 sand, 10 background) using Smart Segmentation (Image-Pro Premier).

mixture. These are analogous to sherds from separate vessels made from the same batch of clay plus sand temper additive, and they illustrate the variation one might expect in multiple ceramic objects made from the same clay-temper batch.

Results for the two measurement approaches (individually measuring, or using a saved segmentation recipe) are highly correlated (Pearson Correlation Coefficient .995), which clearly indicates that using a saved segmentation recipe on many thin sections can substitute for the time-consuming process of segmenting each and every thin section image (Figure 5). The scatter increases with increasing sand amount, as expected. Overall, the percentages for individually measurement are somewhat lower than for applying the saved recipe, indicating that some sand grains were missed by the individual segmentations involving fewer reference marks. Examination of the segmented images indicated that images segmented via saved recipe were not being over-counted with non-sand areas marked as sand.

To examine this comparison more closely, we computed a new variable, Sand Difference, as percent sand identified via recipe minus percent sand identified via individual segmentation. The frequency histogram for this variable (Figure 6) shows that the segmentation recipe applications gave, on average, slightly higher results. So the approach of selecting about 10-20 reference points on each thin section produces relatively consistent results, but often with slightly lower percentages than those obtained by using one more carefully constructed (40-60 reference points) segmentation recipe in a standard way on all samples of that clay color. Individual segmentation, of course, has the great disadvantages of being much more time-consuming, being prone to occasional errors, and precluding batch processing for handling large numbers of images efficiently.

After several sand and background points have been chosen, the Image-Pro Premier software we use makes it possible to see and monitor which sand points are not yet included (by using a semi-transparent mask for the sand segmentation, step-by-step as it occurs) so that new reference points can be strategically selected. One can also see and monitor the parameters brought into the segmentation recipe at each step. If it becomes apparent that the parameters are no longer changing very much, then it may be that optimal segmentation has already been achieved and reference marking can cease.

Some materials that are more uniform and that have clearly distinct phases may require only a few points for successful segmentation. And, if a material allows one to draw ellipses or circles around a large area for reference marking, rather than having to mark single points, optimal segmentation could be achieved more quickly. But, with the range of subtle variation present in archaeological ceramic samples, the 20-30 points per phase seem to be required most often.

For our method of kneading a loose sand volume into wet clay, the measured area percentage is consistently under the target volume percentage of sand. Comparing our results with the target sand additions indicates that multiplying our measured results by about four-thirds will calibrate to how a potter following this method may have originally measured out a temper additive. But for any statistical analysis, multiplying by a constant factor should make no difference. The discrepancy between target and measured amounts is likely due to the volume of air surrounding the loosely packed sand grains, which is no longer present after kneading. The sand volume also varies, depending on the effort put into tamping down grains. Dry clay can also vary in volume by as much as 30 percent, depending on tamping effort. An additional factor may be that many sand grains in thin section will not be cut through their largest diameter (statistically the average diameter will be .785 times the actual diameter), which can affect area measurements (Stoops 2003).

While for the purpose of this experiment we give results to one decimal place, in reality one can only estimate to 1-2 percent, at best, for volume of sand, due to the shape of the grains (which do not pack consistently). The variation seen from one specimen to another is expected. Whether mixing ingredients dry, wet, or in a combination, perfect homogeneity of sand distribution is impossible to achieve by traditional kneading methods.

For all of the target amounts of added sand, slightly more sand was consistently measured with the white clay than with the red clay (Figure 7). This is partially explained by the data in Table 2 for the specimens with no added sand. Sand impurities in the

TABLE 2. Total Area % of Sand-Sized Particles (≥ .063 mm), All 96 Specimens

Added Sand	Red Clay	White Clay
None	.4	.9
	.3	1.3
	.3	.5
Fine, 10%	6.8	7.7
	8.2	8.0
	6.9	7.8
	7.6	8.1
	6.7	8.2
Medium, 10%	6.4	8.2
	5.2	9.2
	5.9	8.4
	5.9	9.6
	5.9	8.0
Coarse, 10%	8.9	7.2
	9.4	9.5
	5.0	10.2
	2.8	9.4
	8.0	11.9
Fine, 25%	16.0	19.1
	17.0	20.8
	17.7	20.0
	15.6	19.8
	17.7	19.5
Medium, 25%	15.8	20.2
	19.0	21.1
	16.2	20.2
	17.6	21.6
	16.5	22.7
Coarse, 25%	19.6	21.0
	17.3	19.5
	15.4	21.0
	17.7	17.6
	17.7	16.5
Fine, 40%	28.7	32.6
	26.6	30.3
	27.1	34.4
	28.2	30.7
	28.3	32.8
Medium, 40%	35.4	32.9
	35.5	36.3
	33.2	34.5
	31.3	34.7
	30.9	36.2
Coarse, 40%	30.7	33.8
	31.8	33.5
	29.5	27.7
	28.4	31.6
	25.6	31.8

Note: Replicate specimens made from each clay-sand combination; area % determined on an entire scanned thin section (optical resolution 7µm/pixel) using Smart Segmentation (Image-Pro Premier) via saved recipe for each clay type, 40–60 reference points. Added sand target percentages are by volume loose sand kneaded into wet clay. Fine = 70-mesh; medium = 30-mesh; coarse = 16-mesh. Silt-sized quartz particles were filtered out by editing the analysis range to ≥ .063 mm.

clay itself are slightly higher for the white than for the red clay, with the red clay specimens containing an average of .3 percent sand and the white clay specimens an average of .9 percent. But, while the base difference is .6 percent, there is an average measured difference of 2.5 percent, so almost 2 percent of that is unaccounted for. As much as .8 percent of that may be explained by the fact that the red clay has a higher amount of porosity than the white, perhaps due to a difference in shrinkage properties (Reedy et al. 2014). The remaining 1.1 percent difference may be due to differing performance of the segmentation recipes on the two different materials.

For comparison, we analyzed a subset of thin sections using images taken at the microscope, with five fields of view in plane-polarized light under 50x magnification. Because we were measuring only area percentage and not size and shape parameters, grains with touching borders did not have to be excluded. Results of the microscope views were problematic, because there was often much variation from one field of view to another. If one or more large grains happen to be in the field of view, the area percentage is quite high; if the field of view happens to be in an area with few or only very small grains, the percentage is quite low. Because archaeological ceramic materials tend not to be uniform, this may always be the case. To achieve a representative number, one would likely have to follow procedures recommended for sedimentary materials (Layman 2002), including as many as 20-30 images to be averaged, and possibly using a lower power objective (25x magnification). While using a saved segmentation recipe on these images could speed up analysis, it would still be time consuming to systematically mark out 20-30 fields of view, capture the digital images, and analyze them all, or to tile for a single analysis the fields of view representing that amount of area. Using an entire scanned

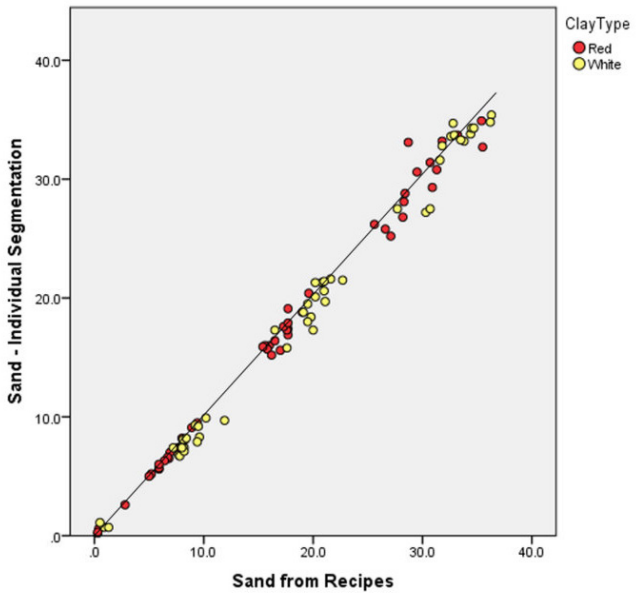

FIGURE 5. Relationship between individually segmenting images (10-20 reference points) and applying a saved recipe (40-60 points) to multiple images shows strong correlation (Pearson's Correlation Coefficient .995), although overall results for individual ones are somewhat lower, implying that some sand grains are missed and the more extensive reference marking used for the recipe captures them.

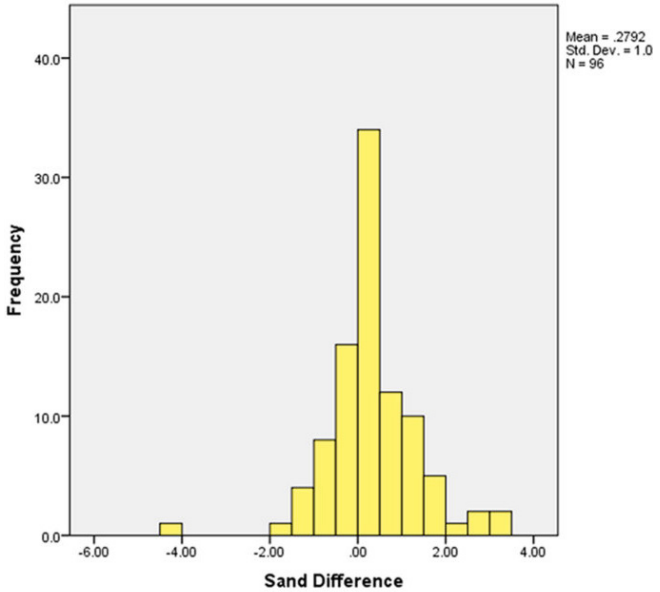

FIGURE 6. Frequency histogram of Sand Difference (% sand identified via recipe minus % sand identified via individual segmentation) shows that recipe applications give, on average, slightly higher results (mean difference < .3%).

thin section instead makes characterizing a large number of thin sections more practical.

ANALYZING COMPLEX ARCHAEOLOGICAL CERAMICS

Characterizing quartz-rich sand temper in ceramics is a relatively easy application of image analysis. While most ceramics do contain quartz sand, many also have considerable amounts of feldspars, iron oxides, micas or other minerals, rock fragments of various types, shell, grog, and/or organic materials. Once we felt comfortable with the workability of the protocols discussed above, we then applied them to a variety of real archaeological specimens representing a full spectrum of materials and temper additives, as well as to a small selection of laboratory-prepared specimens containing some of these additives. In some cases, the protocols could be applied as is; in other cases, additional preprocessing steps or post-segmentation filtering was required in order to correctly segment the phase of interest. If there is a mix of particle types, a series of saved segmentation recipes can analyze them sequentially. Alternatively, one complex segmentation recipe could be used to segment all particle types in one operation, but we find it easier to focus on one at a time in sequence.

Shell

Shell inclusions can have a variety of colors, shapes, and textures. With some examples, we found that Smart Segmentation applied to images of scanned thin sections performed as well as it did with quartz sand. The only preprocessing needed was to apply a "best fit" (to reset black/white levels by averaging the upper and lower levels of all channels). Variables from all three categories (color, background, and morphology) entered into the formulation, and segmentation worked well.

With other examples the solution was more complex. Sometimes, there was a high degree of similarity between the appearance of the shell and of the clay. Sometimes, large shell areas distinct from the clay matrix were lacking, such as when there were many holes in shells where the underlying clay matrix was exposed, or when many small pieces had chipped off of the shells and become well mixed into the clay matrix. In these situations, the scanned image did not always work well, and better performance was achieved by using the automatic tiling feature of Image-Pro Premier to produce an image of a large area of the thin section under magnification, using plane-polarized light. (One could also use multiple fields of view, but then shell pieces on boundaries would have to be excluded for most measurements). Once this image was acquired, preprocessing adjustments were made as follows: (1) "Invert Display" was applied (to create a reversed, or negative, color image, which sometimes makes the phase of interest stand out better); and (2) contrast and gamma were adjusted, again to make the shell stand out more. In Smart Segmentation, the "Background" option was removed from consideration, so that only variables of color and morphology were used. Reference marking took some interactive tweaking, with the original image aligned directly above the one being segmented.

Feldspars

Feldspars are notoriously difficult to segment for image analysis, being colorless like quartz in plane-polarized light, and in crossed-polarized light close to the same birefringence as quartz and often having twinned zones within a single grain that may

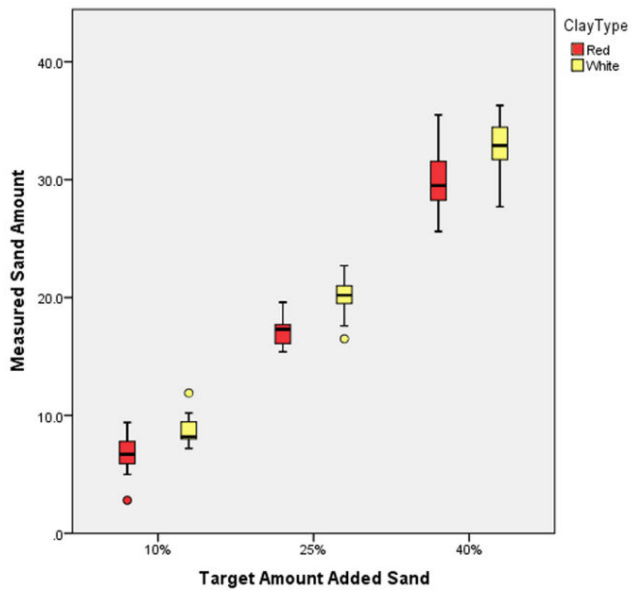

FIGURE 7. Box plot of relationship between measured sand amount and volume percentage loose sand kneaded into clay shows that at all three levels (10, 25, and 40 percent) the means for white clay are slightly higher than for red clay. Brackets mark upper and lower ranges, and colored areas the interquartile range occupied by 50 percent of the numbers. Outliers are separately marked.

be classified by image analysis as different grains. Various solutions have been tried in the past, including combining images taken at the microscope with plane-polarized light, crossed-polarized light, and crossed-polarized light with a gypsum plate (Whitbread 1991); and doing automated gray-level processing under different orientations of cross-polarization (Smith and Beermann 2007).

Using crossed-polarized light images for analysis is always problematic because many grains (feldspar, quartz, etc.) are in extinction and so dark and not discernible, and pores are also difficult to pick out. Given the ability of the Smart Segmentation procedure to incorporate a variety of data, we found that a good approach is to utilize the tendency of feldspars to appear cloudy or dusty in plane-polarized light, due to the formation of alteration productions. In contrast, quartz is not easily affected by alteration and hence tends to remain clear (Kerr 1977) (Figure 8). Once microscopy has identified the presence of feldspars in a sample, the contrast between cloudy feldspars and clear quartz grains can be enhanced through preprocessing, using either a scanned or tiled image. The exact procedure to use depends on the appearance of the clay matrix in contrast to the feldspar grains, but we found several procedures that worked well over a range of specimens:

- As with some of the shell objects discussed above, we adjusted for "best fit," and then simply adjusted brightness, contrast, and gamma until the altering feldspars were distinct from the clear quartz and the clay matrix. Marking reference areas was then easier, and segmentation worked well (Figure 8).
- For some specimens, reference marking was easier if we did preprocessing by beginning with a "best fit," then "inverting display," followed by adjusting brightness and gamma.
- Some examples worked best by beginning the preprocessing with an HSI saturation adjustment (extracting a gray-scale image representing the saturation channels from the color image), followed by adjusting brightness and gamma as needed.

An alternative approach could be to use thin sections that have been stained for plagioclase (red or pink) and potassium feldspar (yellow), using potassium rhodizonate, sodium cobaltinitrite, and barium chloride. However, the stains are often rather pale and subtle, or are uneven and spotty. The more calcic plagioclases will stain more deeply, and pure sodic albite will not stain at all. The accuracy of the stain also decreases with finer grain sizes. So, while staining can help in identifying the minerals, the stains may not work better for image analysis than does the cloudy and dusty appearance of the feldspars. We have, however, had some success using the inverted display image in preprocessing, which made the differences highlighted by the stains stand out better for reference marking.

Rock Fragments

A wide range of rock fragments may be encountered in ceramics, so the protocols necessary for segmentation will vary. We found that some fragments—for example, olivine basalt and many limestones—are easily segmented using the same protocols as for quartz sand, with either no preprocessing or with minor adjustments. Calcium carbonate fragments can be further highlighted by staining, making reference marking easier. Alizarin Red S stains carbonates red. Granitic fragments comprised of quartz and feldspars pose the biggest difficulty, as quartz and feldspars may also come with sand, or may break off from rock fragments. In this case, post-segmentation filtering by size range would usually serve to separate the rock fragments, as they tend to be much larger. To measure and count rock fragments, one would want to segment the quartz and feldspar as a single component. However, for some approaches to petrography, as with the Gazzi-Dickinson method of point counting (Dickinson 1970; Gazzi 1966; Heidke and Miksa 2000; Lombard 1987), the analyst may choose to separately segment and count the minerals within granitic fragments, in which case the methods discussed above for separating quartz from feldspars would be applied. Argillaceous rock fragments would be treated similarly to grog (see below), which they greatly resemble.

Micas

Brown/yellow/green micas such as biotite and chlorite are easily distinguishable for image analysis. However, colorless micas such as muscovite at first appeared to be problematic, as they are colorless and clear like quartz in plane-polarized light. In crossed-polarized light, while often distinctly colored, many minerals such as micas go in and out of darkness (extinction) as the microscope stage is rotated and can also have a birefringence color range that is quite variable, even within a single grain. However, we found that a procedure that works quite well is to reference mark all the colorless quartz and mica grains in a scanned thin section together as one phase for initial segmentation. Then, for obtaining post-segmentation measurement data, we edit the aspect ratio range (ratio between the major axis and

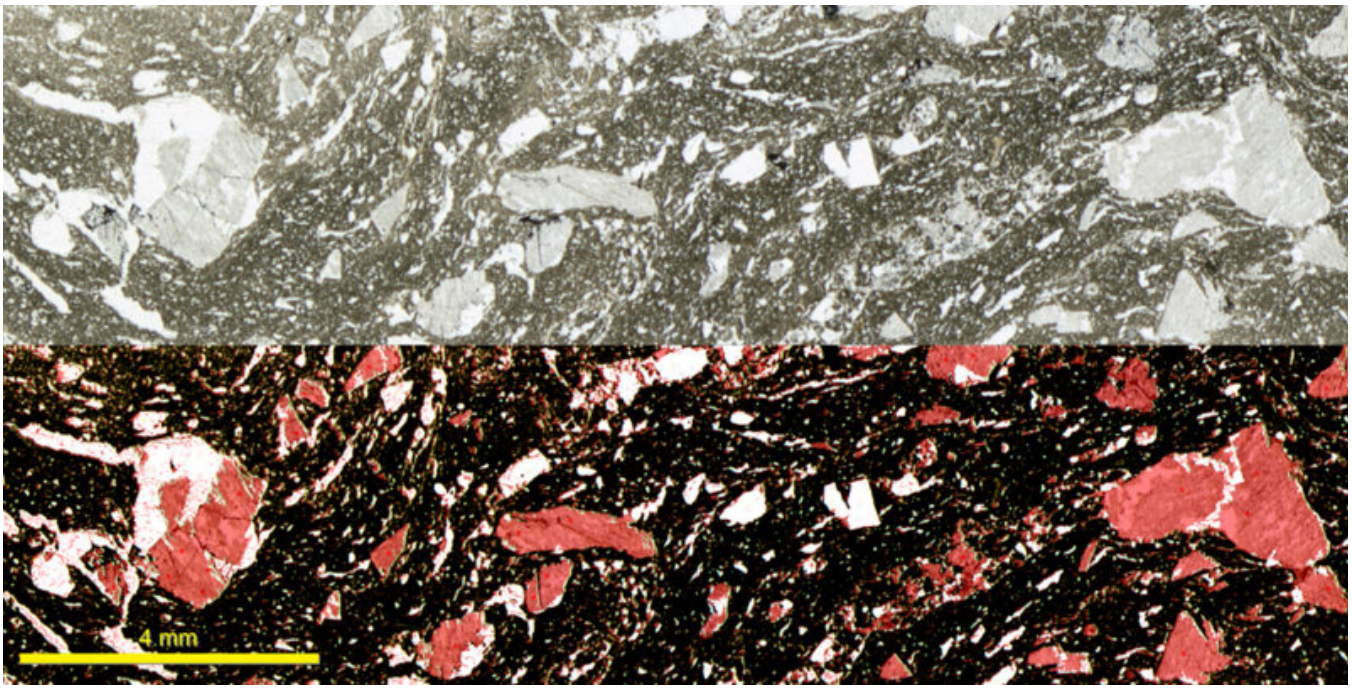

FIGURE 8. Scanned thin section (NA2, Owasco corded ware, Susquehanna Valley, Pennsylvania, 900–1200 A.D.). Top: granitic rock fragments and loose grains within the clay matrix show contrast between clear quartz and cloudy, altered feldspars. Bottom: segmentation of feldspars based on clear vs. cloudy texture.

minor axis of grains) to filter out the quartz grains and count only the mica grains. This works because the micas are usually more elongated, occurring as tabular crystals or shreds. In contrast, quartz occurs in prismatic crystals, which in clay and sands may become rounded and in prepared tempers may be angular. Setting the aspect ratio to a minimum of 2.0 usually works to remove quartz and leave the muscovite (or other clear mica) to be counted, although that might differ somewhat for different materials. Checking some grains seen on the scanned image with their identifications under the microscope helps to ensure that the best aspect ratio is selected.

Grog and ARF

Grog (crushed sherds) and argillaceous rock fragments (ARF) (Whitbread 1986) are perhaps the most problematic materials to segment for image analysis in ceramics. Discerning grog or ARF from the clay matrix is straightforward when there are strong color and textural differences between fragments and the surrounding matrix; however, sometimes they are very similar. Adding to the difficulty is that sometimes there are inclusions of quartz or other minerals within the fragments, and these may be similar to inclusions found throughout the ceramic matrix. We found some success using the preprocessing steps mentioned above for ceramics with shell or feldspars, adjusting for "best fit" (resetting black/white levels), then "inverting display" to create a negative image, followed by adjusting brightness and gamma. But finding an adequate segmentation recipe was sometimes difficult and took much iterative work alongside the original image; it may also work better with a tiled microscopic view, rather than a scanned image. This is certainly a case where the effort to develop a good segmentation recipe is worthwhile if there are many similar specimens that will then be analyzed with the same one. If there are only a few thin sections to analyze, traditional methods of microscopy might be a better use of time and effort.

Metal Oxides

Hematite is a common constituent of ceramics fired under oxidizing conditions. In thin section, it appears as deep red-brown opaque chunks ranging in size from tiny to massive, very red along thin edges. Standard preprocessing steps mentioned above work well for segmenting hematite in image analysis: (1) simply adjusting brightness, contrast, and gamma until the hematite stands out well for reference marking usually suffices and; (2) inverting display works even better at causing the hematite to stand out from reddish iron-rich clay while also clearly distinguishing it from other minerals.

Common opaque black metal oxides include magnetite and ilmenite. They may be distinguished from each other by shape (with magnetite in triangular, square, or rhombic sections, and ilmenite in tabular crystals with elongate sections or in irregular masses). The only other component they can be confused with in segmentation is charred organic material, if this is also present. This can be compensated for by letting all black areas be segmented, then, as with micas, obtaining post-segmentation measurement data only on the metallic oxides present by editing size and/or shape characteristics (depending on the characteristics of those minerals and the organics in a particular set of specimens), so that only the phase of interest will be included. Alternatively, a tiled image for analysis can be constructed of the specimen under reflected light microscopy, where metal oxides may be distinguished from each other and from charred organics by differences in color and metallic luster.

Organic Materials

Organic materials, such as straw or chaff, that do not burn out during firing can range from a deep brown or brownish-orange to black and may have very distinct shapes, although charring can cause small pieces to flake off into the matrix. We found that a preprocessing procedure with excellent results was to invert display, since that made organic materials, dark clays, sand, and pores more clearly distinct, resulting in good segmentation for image analysis.

CONCLUSIONS

Image analysis, as applied to optical microscopy, is a relatively new tool that can augment the existing toolkit of thin-section petrography of archaeological ceramics. While some efforts have gone into trying to automate mineral identification, that is not an avenue that appears to be very satisfactory or useful. Examination under a microscope by a trained petrographer is likely to always be important for the study of ceramic materials. However, image analysis can enhance ceramic studies by providing a variety of quantitative parameters; these measurements can include a comprehensive suite of data for a large number of grains collected relatively quickly for statistical comparisons that can enrich archaeological research, particularly for studies involving technological characterization, grouping, or provenance studies of ceramic materials.

This study focused on checking the consistency and reliability of the measurement of aplastic inclusions in ceramics, as well as establishing some workable methods and protocols. Starting with simple clay-sand systems, we found protocols that provided consistent and reproducible results for segmenting the sand. With the addition of simple preprocessing or post-segmentation filtering steps as needed, these protocols proved useful for a variety of ceramic types beyond the simple clay-sand systems. Images of entire thin sections obtained from a high-resolution film scanner could be used in most cases. The advantage of collecting statistical data on scanned thin sections is that all of the features, even very large grains, are present in their entirety, and data can be obtained on hundreds or even thousands of grains at once. For some materials, a tiled image that incorporates a large area of the thin section under magnification of a low-power objective may be necessary. If multiple fields of view under the microscope are used instead, then objects touching borders must be excluded from most measurements. Mounting thin sections in a dyed epoxy makes distinguishing pores from colorless minerals possible.

While we chose a comprehensive state-of-the-art commercial image analysis package (Image-Pro Premier), it is possible that similar results could be obtained from other image analysis programs. A feature we found crucial to success was the ability of the Smart Segmentation procedure in Image-Pro Premier to incorporate a wide range of parameters into segmentation recipes. Many segmentation procedures use only selected color or gray-scale data. Quartz sand grains may be adequately segmented using only RGB (Red-Green-Blue color model) parameters, for example. However, with most of the more complex archaeological specimens, there may be as many as 10-15 color channel and morphological parameters that enter into segmentation. Developing a carefully constructed segmentation recipe is also crucial, so the software's ability to incorporate multiple images into its construction is important when it is impossible to find a single image representing the full range of variation for a set of specimens. Being able to save a segmentation recipe and apply it to multiple thin sections is crucial for being able to process large numbers of specimens for statistical analysis. Another feature that an image analysis program should include is the ability to conduct a wide range of preprocessing and post-segmentation filtering procedures, as needed. Its image capture parameters should also include live, extended depth-of-field corrections (for ease of producing very well-focused images, a requirement of effective image analysis, especially for fine-grained ceramics), as well as live tiling of a large section of the thin section under magnification, to avoid many grains touching borders on smaller fields of view.

One example of how we have begun to routinely incorporate image analysis into thin-section petrography of ceramic materials is a study of sherds of high-fired glazed ceramics produced by four Song Dynasty kiln groups in China that served the needs of the Imperial Palace (Ru and Jun in Henan Province, Ding in Hebei Province, and Guan, which moved from Henan to Zhejiang Province). The project is being done in conjunction with the Key Scientific Research Base of Ancient Ceramics of the State Administration for Cultural Heritage, Research Laboratory of Ancient Ceramics, Palace Museum, Beijing, which provided sherds from their archaeological collections. The aims of this research are to assess technological variation within a kiln group, to compare technological features of different kiln groups, and to identify technological characteristics of high-quality products vs. misfired ones.

While minerals of the ceramic bodies and glazes are identified through traditional microscopy, quantitative data for statistical analyses is collected via image analysis. Thin sections are first prepared using a dyed epoxy and are examined under the microscope to identify minerals present in the body, glaze layers, and body-glaze interface. Thin sections are then scanned (at 5300 x 5300 ppi). A polygon is drawn around the ceramic body to separate it from glaze layers, and it is saved as a Region of Interest (ROI) (Figure 9). This ROI is used for image analysis that records area percentage of pores, sand, and any other major components present. A suite of quantitative measurements (length/feret diameter, area, perimeter, aspect ratio, roundness, and circularity) are recorded for sand-sized quartz grains (≥ .063 mm) and for pores ≥ .063 mm. Minimum, maximum, and average thicknesses are measured for the ceramic body, the glaze, and any slip or glaze-body interaction zones present. ROIs are drawn around each glaze layer to measure area percentage and size of bubbles and larger crystals in the glaze. Quantitative data from image analysis is combined with qualitative mineralogical information (presence/absence) for statistical analyses that examine variation within and between kiln groups. Combining the image analysis data with the more traditional qualitative data helps to better characterize each kiln group and identify differences between them.

Each group of archaeological ceramics will likely require slightly different preprocessing methods to best separate components of interest and background, will have different parameters that enter into the segmentation recipe, may need somewhat different post-segmentation filtering procedures to ensure that only

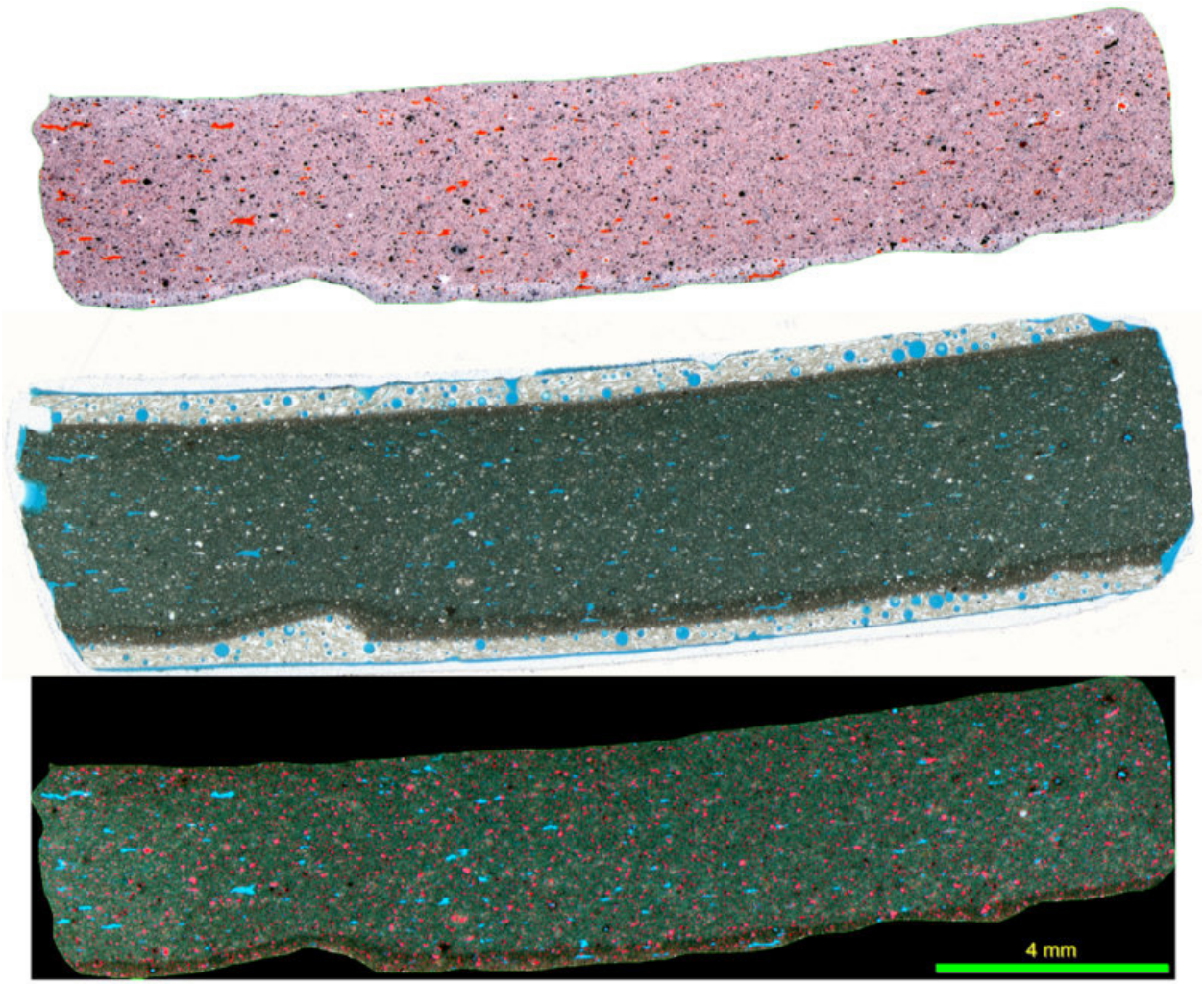

FIGURE 9. Scanned thin section from Imperial-quality Ru ware sherd (Ru-5, Qingliangsi, Baofeng County, Henan Province, China, Song Dynasty). Center: Thin section as scanned, showing dense gray body with inner and outer glaze layers. Bottom: region of interest (ROI) drawn to exclude all but ceramic body from segmentation and measurement of particles (3.3 % fine sand .063–.2 mm, no grains of sand above .2mm, and 8 percent silt-sized particles < .063 mm). Top: inverted display (negative) image used to segment pores for measurement, 2.1 percent.

the phase of interest is measured, and will collect data on a different set of measurements, depending upon the nature of the ceramic material and the research questions of interest. Nonetheless, there are some clear guidelines that can be followed to ensure that image analysis can be used in an efficient, reliable, and consistent manner to augment traditional methods of thin-section petrography in studies of archaeological ceramics.

Acknowledgments

This work was supported by National Science Foundation grant 1005992. Pamela Vandiver, University of Arizona, kindly provided some of the archaeological ceramics examined to extend our range of specimens.

Data Availability Statement

All of the images used in the experimental section are available at the University of Delaware Library's Institutional Repository (UDSpace) (under the Center for Historic Architecture and Design documents, sub-community Laboratory for Analysis of Cultural Materials, http://udspace.udel.edu/handle/19716/12425) and can be downloaded by anyone interested in experimenting with image analysis. The collection is titled Ceramic Image Analysis—Laboratory-Prepared Specimens. Selecting "Titles" shows all of the available images. These are listed by type of clay (red or white), percentage of added sand, and size category of sand (coarse, medium, or fine). All specimens include scanned thin sections, with replication. Many also include surface images taken under a stereomicroscope, and individual fields of view taken under a polarizing microscope. Some additional archaeological specimen images, along with their image analysis results, are also available under the collection title: Ceramic Image Analysis—Archaeological Specimens. More are in the process of being added. The thin sections that were scanned to produce all images in the UDSpace collections are available by appointment to study in UD's Laboratory

for Analysis of Cultural Materials. Contact information: Chandra L. Reedy, clreedy@udel.edu; 240 Academy Street, University of Delaware, Newark, DE 19716.

REFERENCES CITED

Arnold, Dean E.
1972 Mineralogical Analyses of Ceramic Materials from Quinua, Department of Ayacucho, Peru. *Archaeometry* 14:93-102.

Bouchain, Isabelle, and Bruce Velde
2001 Grain Distribution by Image Analysis of Thin Sections in Some Gaulo-Roman Common Ware, St. Marcel (Indre) France. In *Archaeology and Clays*, edited by Isabele C. Druc, pp. 71-80. British Archaeological Reports, Oxford.

Coster, Michel, and Jean-Louis Chermant
2001 Image Analysis and Mathematical Morphology for Civil Engineering Materials. *Cement & Concrete Composites* 23:133-151.

Cox, Melissa R., and Muniram Budhu
2008 A Practical Approach to Grain Shape Quantification. *Engineering Geology* 96:1-16.

Day, Peter M., and David E. Wilson
1998 Consuming Power: Kamares Ware in Protopalatial Knossos. *Antiquity* 72:350-358.

De Keyser, Thomas L.
1999 Digital Scanning of Thin Sections and Peels. Research Methods Papers. *Journal of Sedimentary Research* 69:962-964.

Dickinson, William R.
1970 Interpreting Detrital Modes of Graywacke and Arkose. *Journal of Sedimentary Petrology* 40:695-707.

Dickinson, William R., and Richard Shutler Jr.
1979 Petrography of Sand Tempers in Pacific Islands Potsherds: Summary. *Geological Society of America Bulletin* 90:993-995.

Fieller, Nicholas R. J., and Paul T. Nicholson
1991 Grain Size Analysis of Archaeological Pottery: The Use of Statistical Models. In *Recent Developments in Ceramic Petrology*, edited by Andrew Middleton and Ian Freestone, pp. 71-111. British Museum, London.

Forte, Maurizio
1994 Archaeometric and Digital Computer Analysis on Etruscan Bucchero from Marzabotto. In *The Ceramics Cultural Heritage: Proceedings of the International Symposium of the 8th CIMTEC World Ceramic Congress and Forum on New Materials*, edited by Pietro Vincenzini, pp. 529-39. TECHNA, Faenza.

Francus, Pierre
1998 An Image Analysis Technique to Measure Grain-size Variation in Thin Sections of Soft Clastic Sediments. *Sedimentary Geology* 121:289-298.

Freestone, Ian C.
1995 Ceramic Petrography. *American Journal of Archaeology* 99:111-117.

Freestone, Ian C., Catherine Johns, and Tim Potter (editors)
1982 *Current Research in Ceramics: Thin-Section Studies.* British Museum Research Laboratory, London.

Gazzi, Paolo
1966 Le Arenarie del Flysch Sopracretaceo dell'Appennino Modenese: Correlazioni con il Flysch di Monghidoro. *Mineralogica e Petrografica Acta* 12:69-97

Hansen, Eric F.
2000 *Ancient Maya Burnt-lime Technology: Cultural Implications of Technological Styles.* Ph.D. dissertation, Archaeology Program, University of California, Los Angeles. University Microfilms, Ann Arbor.

Heidke, James M., and Elizabeth J. Miksa
2000 Correspondence and Discriminant Analysis of Sand and Sand Temper Compositions, Tonto Basin, Arizona. *Archaeometry* 42(2):273-299.

Hutchison, Charles S.
1974 *Laboratory Handbook of Petrographic Techniques.* John Wiley & Sons, New York.

Kerr, Paul F.
1977 *Optical Mineralogy.* McGraw Hill, Boston.

Layman, John M., II
2002 *Porosity Characterization Utilizing Petrographic Image Analysis: Implications for Identifying and Ranking Reservoir Flow Units, Happy Spraberry Field, Garza County, Texas.* Master's thesis, Geology Department, Texas A & M University.

Leese, Morven N.
1983 The Statistical Treatment of Grain Size Data from Pottery. In *Proceedings of the 22nd Symposium on Archaeometry*, edited by Arnold Aspinall and Stanley E. Warren, pp. 47-55. University of Bradford.

Livingood, Patrick C.
2007 Plaquemine Recipes: Using Computer-Assisted Petrographic Analysis to Investigate Plaquemine Ceramic Recipes. In *Plaquemine Archaeology*, edited by Mark A. Rees and Patrick C. Livingood, pp. 108-126. University of Alabama Press, Tuscaloosa.

Livingood, Patrick C., and Ann Cordell
2009 Point/Counter Point: The Accuracy and Feasibility of Digital Image Techniques in the Analysis of Ceramic Thin Sections. *Journal of Archaeological Science* 36: 867-872.
2014 Point/Counter Point II: The Accuracy and Feasibility of Digital Image Techniques in the Analysis of Pottery Tempers Using Sherd Edges. In *Integrated Approach in Ceramic Petrography*, edited by Mary F. Ownby, Maria Masucci, and Isabelle Druc. University of Utah Press, Salt Lake City, in press.

Lombard, James P.
1987 Provenance of Sand Temper in Hohokam Ceramics, Arizona. *Geoarchaeology* 2(2): 91-119.

Matthew, A. J., Ann J. Woods, and C. Oliver
1991 Spots Before the Eyes: New Comparison Charts for Visual Percentage Estimation in Archaeological Material. In *Recent Developments in Ceramic Petrology*, edited by Andrew Middleton and Ian Freestone, pp. 211-263. British Museum Occasional Paper No. 81. British Museum Research Laboratory, London.

Middleton, Andrew P., Ian C. Freestone, and Morven N. Leese
1985 Textural Analysis of Ceramic Thin Sections: Evaluation of Grain Sampling Procedures. *Archaeometry* 27(1):64-74.

Middleton, Andrew, and Ian C. Freestone (editors)
1991 *Recent Developments in Ceramic Petrology.* British Museum Occasional Paper No. 81. British Museum Research Laboratory, London.

Miriello, Domenico, and Gino Mirocle Crisci
2006 Image Analysis and Flatbed Scanners. A Visual Procedure in Order to Study the Macro-porosity of the Archaeological and Historical Mortars. *Journal of Cultural Heritage* 7:186-192.

Nijboer, Albert J., Peter A. J. Attema, and Gert J. M. Van Oortmerssen
2006 Ceramics from a Late Bronze Age Saltern on the Coast Near Nettuno (Rome, Italy). *Palaeohistoria* 47/48:141-205.

Norbury, David
2010 *Soil and Rock Description in Engineering Practice.* Whittles, Dunbeith, Scotland.

Orton, Clive
2000 *Sampling in Archaeology.* Cambridge University Press, Cambridge.

Peacock, David P. S.
1970 The Scientific Analysis of Ancient Ceramics: A Review. *World Archaeology* 1:375-389.

Persson, Anna-Lena
1998 Image Analysis of Shape and Fine Aggregates. *Engineering Geology* 50:177-186.

Pettijohn, Francis J.
1975 *Sedimentary Rocks.* 3rd ed. Harper and Row, New York.

Protz, R., and A. J. VanderBygaart
1998 Towards Systematic Image Analysis in the Study of Soil Micromorphology. *Sciences of Soils* 3:34-44.

Quinn, Patrick S. (editor)
2009 *Interpreting Silent Artefacts: Petrographic Approaches to Archaeological Materials*. Archaeopress, Oxford.

Quinn, Patrick S.
2013 *Ceramic Petrography: The Interpretation of Archaeological Pottery & Related Artefacts in Thin Section*. Archaeopress, Oxford.

Reedy, Chandra L.
2006 Review of Digital Image Analysis of Petrographic Thin Sections in Conservation Research. *Journal of the American Institute for Conservation* 45:127-146.
2008 *Thin-Section Petrography of Stone and Ceramic Cultural Materials*. Archetype, London.
2012 Image Analysis-Aided Light Microscopy of Glazed Ceramics: Identifying Technological Innovation and Style. *Studies in Conservation* 57(S1):227-233.

Reedy, Chandra L., Jenifer Anderson, and Terry J. Reedy
2014 Quantitative Porosity Studies of Archaeological Ceramics by Petrographic Image Analysis. In *Materials Issues in Art and Archaeology X*, edited by Pamela B. Vandiver, Weidong Li, Phillip Sciau, and Christopher Maines. Cambridge University Press, in press.

Reedy, Chandra L., and Sachin Kamboj
2003 Comparing Comprehensive Image Analysis Packages: Research with Stone and Ceramic Thin Sections. In *Development of a Web-Accessible Reference Library of Deteriorated Fibers Using Digital Imaging and Image Analysis*, edited by Jane Merritt. National Park Service, Harpers Ferry, West Virginia, 159-166.

Rice, Prudence
1987 *Pottery Analysis: A Sourcebook*. University of Chicago Press, Chicago.

Russ, John C.
2011 *The Image Processing Handbook*. CRC, Boca Raton, Florida.

Rye, Owen S.
1976 Keeping Your Temper under Control: Materials and the Manufacture of Papuan Pottery. *Archaeology and Physical Anthropology in Oceania* 11:106-137.

Schäfer, Michael
2002 Digital Optics: Some Remarks on the Accuracy of Particle Image Analysis. *Particle and Particle Systems Characterization* 19:158-168.

Schäfer, Andreas, and Thomas Teyssen
1987 Size, Shape and Orientation of Grains in Sand and Sandstones—Image Analysis Applied to Rock Thin-Sections. *Sedimentary Geology* 52:251-171.

Schmitt, Anne
1993 Apports et limites de la petrographie quantitative: Application au cas des amphores de Lyon. *Review d'Archéométrie* 17:51-63.

Shepard, Anna O.
1971 *Ceramics for the Archaeologist*. Originally published 1956, Publication 609, Carnegie Institute, Washington, D.C.

Smith, John V., and Eberhard Beermann
2007 Image Analysis of Plagioclase Crystals in Rock Thin Sections Using Grey Level Homogeneity Recognition of Discrete Areas. *Computers and Geosciences* 33:335-356.

Stoltman, James B.
1989 A Quantitative Approach to the Petrographic Analysis of Ceramic Thin Sections. *American Antiquity* 54:147-160.
2001 The Role of Petrography in the Study of Archaeological Ceramics. In *Earth Sciences and Archaeology*, edited by Paul Goldberg, Vance T. Holliday, and C. Reid Ferring, pp. 297-326. Kluwer/Plenum, New York.

Stoops, Georges
2003 *Guidelines for Analysis and Description of Soil and Regolith Thin Sections*. Soil Science Society of America, Madison, Wisconsin.

Streeten, Anthony D. F.
1982 Textural Analysis: An Approach to the Characterization of Sand-tempered Ceramics. In *Current Research in Ceramics: Thin-Section Studies*, edited by Ian C. Freestone, Tim Potter, and Catherine Johns, pp. 123-134. British Museum, London.

Tafesse, Solomon, Joanne M. Robison Fernlund, Wenjuan Sun, and Fredrik Bergholm
2013 Evaluation of Image Analysis Methods Used for Quantification of Particle Angularity. *Sedimentology* 60:1100-1110.

Tarquini, Simone, and Pietro Armienti
2003 Quick Determination of Crystal Size Distribution of Rocks by Means of a Color Scanner. *Image Analysis and Stereology* 22:27-34.

Udden, Johan A.
1914 Mechanical Composition of Clastic Sediments. *Geological Society of America Bulletin* 25:655-744.

Van Den Berg, Elmer H., Victor F. Bense, and Wolfgang Schlager
2003 Assessing Textural Variation in Laminated Sands Using Digital Image Analysis of Thin Sections. *Journal of Sedimentary Research* 73:133-143.

Velde, Bruce, and Isabelle. C. Druc
1999 *Archaeological Ceramic Materials: Origin and Utilization*. Springer, Berlin.

Wentworth, Chester K.
1922 A Scale of Grade and Classifications for Clastic Sediments. *National Research Council Bulletin* 30:377-392.

Whitbread, Ian K.
1986 The Characterisation of Argillaceous Inclusions in Ceramic Thin Sections. *Archaeometry* 28(1):79-88.
1991 Image and Data Processing in Ceramic Petrology. In *Recent Developments in Ceramic Petrology*, edited by Andrew Middleton and Ian Freestone, pp. 369-386. British Museum Occasional Paper No. 81. British Museum Research Laboratory, London.
1995 *Greek Transport Amphorae: A Petrological and Archaeological Study*. Fitch Laboratory Occasional Paper, 4. British School at Athens.

Williams, David F.
1983 Petrology of Ceramics. In *The Petrography of Archaeological Artefacts*, edited by David R. C. Kempe and Anthony P. Harvey, pp. 301-329. Clarendon Press, Oxford.

Wolf, Sophie
2002 Questions, Answers, and Limitations: Chemical, Mineralogical, and Petrographic Distinction between Three Medieval Brick Productions in Switzerland. In *Archaeometry 98*, edited by Erzsebet Jeremy, Katalin T. Biró, and Edina Rudner, pp. 256-261. British Archaeological Reports International Series No. 1043 (II), Archaeolingua, Central European Series No. 1. Archaeopress, Oxford.

ABOUT THE AUTHORS

Chandra L. Reedy ■ Center for Historic Architecture & Design, University of Delaware, 240 Academy Street, 331 Alison Hall, Newark, DE 19716 (clreedy@udel.edu)

Jenifer Anderson ■ Center for Historic Architecture & Design, University of Delaware, Newark, DE 19716; and Historic Sugartown Inc., Malvern, PA 19355

Terry J. Reedy ■ Independent Statistical Consultant, Newark, DE 19711

Yimeng Liu ■ Center for Historic Architecture & Design, University of Delaware, Newark, DE 19716; and China Railway Construction Corporation (International) Ltd., Beijing 100855 P. R. China